

# Design and Development of a Dynamically-Balancing Holonomic Robot

Saul Reynolds-Haertle   Mike Stilman

**Abstract**—This paper describes the design, control, and construction of Golem Wing, the first vehicle which both balances dynamically and has entirely holonomic ground movement. A nonstandard linear arrangement of mecanum wheels gives it the load-lifting, performance, and manipulation benefits of a dynamically-balancing platform without the maneuvering difficulties exhibited by previous balancing platforms. We show that the arrangement is capable of holonomic motion, describe a controller that maintains dynamic balance during holonomic motion, and show an implementation of the system in hardware that validate our assertions.

## I. INTRODUCTION

Dynamically-balancing vehicles are in many ways more capable than statically-stable platforms of the same size and mass; however, they have limited maneuverability. Holonomic vehicles are sufficiently maneuverable, but require a low center of mass, widely-spaced contact points and must be driven relatively slowly to avoid tipping. We developed Golem Wing, a novel vehicle that combines the advantages of these two types of platforms and minimizes their disadvantages. The dynamically-balancing vehicle’s most significant challenge, its lack of maneuverability, is counteracted by the ability to maneuver holonomically. The holonomically-moving vehicle’s drawbacks, including wide wheelbase, low center of mass, and slow movement, are counteracted by the vehicle’s ability to dynamically stabilize its center of mass above the wheel axle.

Dynamic balance is desirable for a number of reasons. Most importantly, dynamically balancing vehicles can handle significantly larger loads relative to their mass [13, 14]. Dynamic balancers keep the greatest forces pointed directly into the floor along the contact line, so adding to or raising the load does not introduce any additional danger of tipping when moving. Dynamic platforms are also much stronger when used for mobile manipulation, since a dynamically-balancing platform can use mechanical advantage to transform potential energy stored in an elevated mass into useful work.

Omnidirectional navigation is also clearly advantageous. Most importantly, it simplifies movement in tight spaces, both for computerized motion planners and human operators. Consider the common case of parallel parking; for nonholonomic platforms such as cars or balancing robots with dual laterally displaced wheels, this is a nontrivial exercise in planning and is occasionally difficult even for experienced human drivers. Holonomic vehicles can achieve instantaneous velocity in any direction, allowing them to

The authors are affiliated with the Center for Robotics and Intelligent Machines (RIM) at the Georgia Institute of Technology, Atlanta, Georgia 30332, USA. Emails: saulrh@gatech.edu, mstilman@cc.gatech.edu



Fig. 1. Golem Wing, a prototype of the novel vehicle arrangement discussed in this paper, with labeled parts.

slide into spaces quickly and without any multi-stage planning such as parallel parking. Similar benefits are found when using human machinery, since most workflows depend on the operator’s ability to sidestep easily. A kitchen may require the cook to slide back and forth between adjacent countertops and stovetops, and a machine shop could require the machinist moving between a machine and a toolbox or between different machines.

We claim that both balance and holonomic motion can be achieved simultaneously. In order to validate our assertions, we constructed a vehicle which uses a novel wheel configuration, named Golem Wing. We use Golem Wing to demonstrate that our wheel arrangement produces holonomic movement and that the vehicle can maintain its balance while moving in any direction. In this paper we describe Golem Wing’s design and construction, derive the inverse kinematic solution for holonomic navigation and combine the inverse kinematic solution with a PID controller that balances the vehicle without restricting movement. We present experimental results showing holonomic movement during dynamic balance on the real robot platform.

## II. RELATED WORK

### A. Dynamically stable vehicles

There exist numerous dynamically-stable vehicles built with laterally displaced wheels; examples include [1, 6, 7, 13, 14]. To our knowledge, all of these vehicles are nonholonomic; however, they share certain advantages. Grasser’s JOE [6]

was constructed using inexpensive off-the-shelf digital signal processing components. The Segway HT and PT demonstrate the load-carrying capacity of dynamically-stable vehicles, being able to safely and stably carry a 125kg load at more than 6 meters per second despite massing only 50kg itself. The UBot [14] showed that dynamically stable robots could push more mass without losing balance. Our earlier work on Sparky [13] investigated contact placement and torque selection to maximize the force capabilities of articulated balancing robots. Furthermore, our work on Golem Krang [22], a human-scale balancing mobile manipulator, has applied stochastic optimization to autonomously generate optimized whole-body motions that take advantage of potential energy and momentum [21].

### B. Holonomic vehicles

Holonomic vehicles are a popular topic in robotics literature and appear in several commercial products. There are several technologies that allow a vehicle arbitrary directional and rotational control. One design uses powered casters that are rotated to face the direction of movement; examples of this design include [24] and [11]. Another design uses three or more Swedish or Mecanum wheels. These wheels have small, freely-rotating rollers mounted around the edge of larger, powered wheels. Examples of this design are found in [2], [20], and [25]. Because of their flexibility in comparison with other omnidirectional technologies, we chose Mecanum wheels to implement our own novel mobile robot.

### C. Omnidirectional dynamically-stable vehicles

There do exist vehicles which are both dynamically stable and capable of achieving instantaneous translational acceleration in any direction. Some balance using one large spherical wheel, as described in [16] and [4]. Others use more esoteric technologies, such as the Honda U3-X. However, these robots are only omnidirectional, *not* holonomic. They can achieve translational acceleration in any direction, but because they have only a single point contact with the ground, they cannot exert torque about a vertical axis and therefore cannot achieve rotational acceleration. In contrast, our robot, Golem Wing, is both dynamically stable and can achieve instantaneous velocities in all translational and rotational directions.

## III. PROTOTYPE: GOLEM WING

We constructed Golem Wing, shown in Figure 1, to validate our assertions about the controllability of the design proposed in this paper. Golem Wing was designed as a minimally complex testbed to demonstrate the controller described in Section IV. The major structural component of the platform is a single eighth-inch aluminum plate, to which three Mecanum wheels (A) are mounted. Note that the rollers of the middle Mecanum wheel are perpendicular to the rollers of the outside wheels; this is necessary for consistent and unique forward and inverse kinematic solutions, as we will show in Section IV-A. The wheels are each powered by one Robotis Dynamixel RX-24F servomotor (B), which behaves as an easily-controllable motor. The mast on the Golem Wing

serves to raise the center of mass and position an IMU and Arduino board (C). The IMU consists of a three-axis accelerometer and one-axis gyroscope. The data is read by an Arduino Pro, and the assembly is placed to avoid being disturbed by the vehicle's oscillations while balancing. The Arduino and servos are tethered (E) to an external control station that includes an 18-volt power supply and a standard Dell laptop. The Arduino sends accelerometer and gyroscope information through the tether to the laptop, which processes the data, runs our controller, and sends commands to the servomotors back through the tether. The accelerometers provide data at 110hz, and the motors receive commands and return state information at 30hz.

## IV. CONTROLLER

### A. Kinematics

Before describing the details of our control system, we first begin by finding a general inverse differential kinematic solution for a vehicle using Mecanum wheels. We assume that no slipping occurs at the contact points between the wheels and the ground. In Section V we will show the resulting solution behaves sufficiently well enough for practical applications.

Referring to Figure 2, the center of the wheel is at  $A = (a_x, a_y)$  relative to the vehicle's center and the angle between the wheel's axis of rotation and the vehicle's x-axis is  $\alpha$ . The angle between the wheel's axis and the axes of the rollers is  $\delta$ . The vehicle frame of reference moves with linear velocity  $V = (v_x, v_y)$  and angular velocity  $\omega$  with respect to the ground. Based on Gferrer [5], we derive the inverse differential kinematics of an arbitrary system of mecanum wheels as follows.

The velocity component of the contact point  $C = (c_x, c_y)$  from the vehicle motion in the universe's frame is

$$V_{C,01} = \begin{pmatrix} v_x - \omega c_y \\ v_y + \omega c_x \end{pmatrix} \quad (1)$$

The velocity component of the contact point from the wheel's motion in the vehicle frame is

$$V_{C,12} = \dot{u} \cdot r \begin{pmatrix} -\sin \alpha \\ \cos \alpha \end{pmatrix} \quad (2)$$

where  $\dot{u}$  is the angular velocity of the wheel. The velocity component of the contact point from the roller spinning is

$$V_{C,23} = \lambda \begin{pmatrix} -\cos \alpha + \delta \\ \cos \alpha + \delta \end{pmatrix} \quad (3)$$

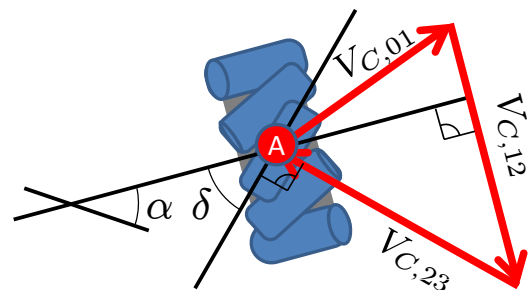


Fig. 2. Velocities for one wheel on a vehicle using Mecanum wheels.

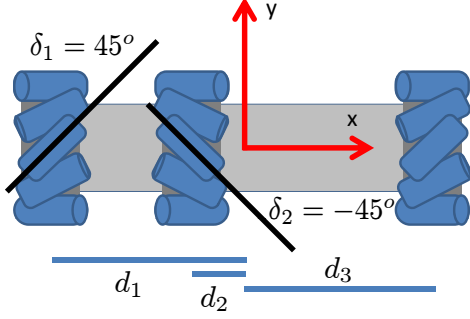


Fig. 3. Kinematic Diagram of the mecanum wheels on Golem Wing. The red lines indicate the vehicle's coordinate system and the black lines indicate the roller angles  $\delta_i$ .

Normally this would be a function of  $u$  as the point of contact moved from side to side across the wheel, but here we make the simplifying assumption that  $C$  lies on the wheel's centerline at all times (that is,  $c_x = a_x$  and  $c_y = a_y$ ). Since we assume the contact patch does not slip, we get:

$$V_{C,01} + V_{C,12} + V_{C,23} = \begin{pmatrix} 0 \\ 0 \end{pmatrix} \quad (4)$$

We solve for  $\dot{u}$ , and the result is the general inverse kinematic solution for a single Mecanum wheel:

$$\dot{u} = -\frac{1}{r \sin \delta} [\sin(\alpha + \delta)(v_y + \omega a_x) + \cos(\alpha + \delta)(v_x - \omega a_y)] \quad (5)$$

This allows us to compute the approximate wheel velocity  $\dot{u}$  for a desired vehicle velocity  $v_x, v_y$  and  $\omega$ . We apply this to each wheel of a vehicle to find the inverse kinematic solution for that vehicle. Applying this to a three-wheeled vehicle yields the following general inverse kinematic solution, with  $c_i$  and  $s_i$  denoting  $\cos(\alpha_i + \delta)$  and  $\sin(\alpha_i + \delta)$ .

$$\begin{pmatrix} \omega_1 \\ \omega_2 \\ \omega_3 \end{pmatrix} = -\frac{1}{r \cdot \sin \delta} \mathbf{M} \begin{pmatrix} v_x \\ v_y \\ \omega \end{pmatrix} \quad (6)$$

$$\mathbf{M} = \begin{pmatrix} c_1 & s_1 & a_{1x}s_1 - a_{1y}c_1 \\ c_2 & s_2 & a_{2x}s_2 - a_{2y}c_2 \\ c_3 & s_3 & a_{3x}s_3 - a_{3y}c_3 \end{pmatrix}$$

The forward kinematics of the system are exactly represented by  $\mathbf{M}^{-1}$ ; if it exists, then regardless of the wheel velocities there is exactly one way the robot can move that will maintain the no-slip assumption. The existence of  $\mathbf{M}^{-1}$  is dependent on the values of  $\alpha$  and  $\delta$ , and Gferrer argues that for a three-wheeled vehicle  $\mathbf{M}^{-1}$  exists as long as the wheel rollers' axes of rotation do not all intersect at the same point and are not all parallel. Note that this is distinct from the axes of the wheels themselves being parallel. Since our wheel arrangement satisfies this condition, Golem Wing has solutions for the forward and inverse differential kinematics that can produce slippless holonomic movement.

### B. Kinematics Examples

In order to more clearly and intuitively illustrate the inverse kinematics of this vehicle, consider a theoretical three-wheeled holonomic vehicle similar in shape (though not in

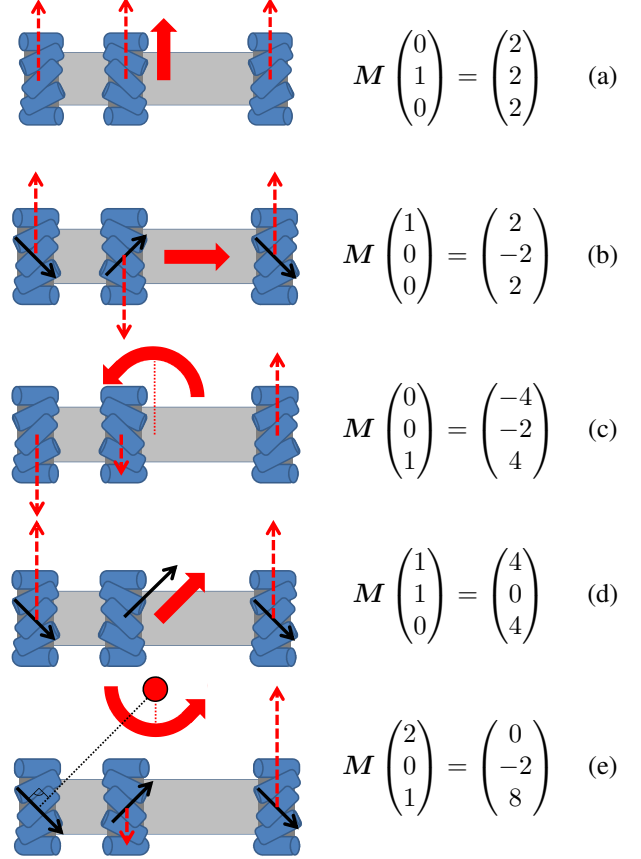


Fig. 4. Examples of interesting kinematic solutions for a theoretical holonomic balancing vehicle. In these figures, the red arrow is the robot's overall motion, the dashed red lines show the motion of each wheel, and the small black arrows show the motion of the rollers on each wheel.

size) to Golem Wing. A kinematic model of this simple vehicle is seen in Figure 3. For this vehicle, the distance from the origin to the two outside wheels (numbers 1 and 3) is  $d_1 = d_3 = 2\text{m}$  and the distance from the origin to the center wheel is  $d_2 = -1\text{m}$ . The rollers on wheels 1 and 3 are both angled at  $\delta_1 = \delta_3 = 45^\circ$  and the rollers on wheel 2 are angled at  $\delta_2 = -45^\circ$ . The wheels themselves have radius  $.5\text{m}$  and are aligned with the  $y$  axes, giving  $\alpha = 90^\circ$ . Applying Eq. 6, then, the inverse kinematics of the example vehicle are:

$$\begin{pmatrix} \omega_1 \\ \omega_2 \\ \omega_3 \end{pmatrix} = \begin{pmatrix} 2 & 2 & -4 \\ -2 & 2 & -2 \\ 2 & 2 & 4 \end{pmatrix} \begin{pmatrix} v_x \\ v_y \\ \omega \end{pmatrix}$$

We now follow the examples shown in Figure 4 (a) through (e). In Figure 4(a), the vehicle wants to move forward at one meter per second, that is,  $v_y = 1\text{m/s}$ . Multiplying the workspace velocity vector by the matrix containing the inverse kinematic solution, we find that  $\omega_1 = \omega_2 = \omega_3 = 2\text{rad/sec}$ . As shown in the figure, this fits perfectly, as all the wheels are parallel and pointing straight forward; the  $.5\text{m}$  wheel radius also matches up properly. In (b), the vehicle is ordered to move directly sideways, that is,  $v_x = 1\text{m/s}$ . Our inverse kinematics tell us that the wheels have velocities

$\omega_1 = 2, \omega_2 = -2, \omega_3 = 2$ . In this case, the contact points on the two outside wheels move down and to the right, while the contact point on the middle wheel moves up and to the right; the rollers on each wheel rotate freely to *absorb* the movement in the y-direction and the vehicle moves in the x-direction only. Rotation around the vehicle’s origin, as shown in (c), is identical to the more common two-wheeled case. Direct diagonal movement, shown in Figure 4(d), is slightly more difficult. In this case, the center wheel stays fixed, since its rollers can follow the desired motion exactly. All of the movement is generated by the outside wheels, whose rollers slowly roll back and to the right to turn the outside wheels’ directly-forward motion into the desired diagonal motion. The final example, rotating around a point directly in front of the robot as shown in Figure 4(d), is the most complex and useful. For instance, a mobile manipulator might use this strategy to circle around an object that’s being manipulated, or to carry a wide object sideways through a sharp corner. In this case, the leftmost wheel’s motion is directly in line with its rollers, as shown by the dashed line indicating that the rollers’ axis of rotation is directly toward the center of the circle the robot describes.

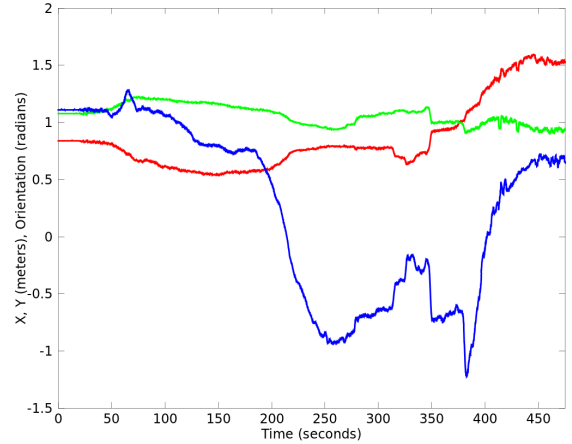
### C. Balancing

The overall controller for the vehicle is a simple PID balancing controller, as found in the majority of dynamically-balancing vehicles, running on top of the inverse kinematic solution from Section IV-A. The inverse kinematics generate a set of wheel velocities that would result in the desired ground motion of the vehicle if followed, which the PID controller uses as reference wheel velocities. Properly chosen PID constants will cause the vehicle to make small, rapid accelerations to maintain balance while the reference inputs from the inverse kinematics drive the vehicle in the desired direction. Many balancing vehicles use identical systems to navigate while balancing, with the difference that their inverse kinematics only allow for medial movement and turning.

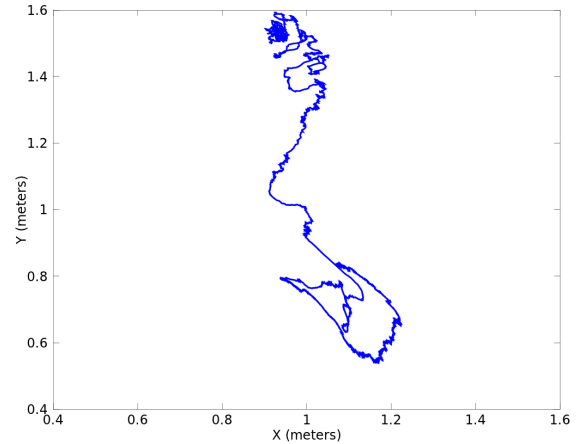
## V. RESULTS

We gathered position and orientation data from Golem Wing using a Polhemus Fastrak 3D magnetic tracking system. Note that we use this sensor *only* for monitoring and data gathering; the robot does not use the tracking system to balance. We present the data gathered during a single run of Golem Wing, covering seven minutes of nearly unassisted balancing during holonomic movement. We show that this data does in fact represent holonomic movement, verifying our claims from earlier sections.

Our raw data has significant noise. The magnetic sensor that we used introduces large, extremely sharp noise into the data, which must be corrected using aggressive smoothing. This noise is at amplitude similar to the movements of the balancing controller, but is at a much higher frequency and can be eliminated using a low-pass filter. In order to preserve smaller movements from the balancing controller, the data in Figure 5 was smoothed using a moving window average



(a) Robot Position and Orientation



(b) Robot Workspace Path

Fig. 5. Plot (a) is a graph of the robot’s position and orientation as a function of time. The green line shows the X-coordinate in meters, the red line the Y-coordinate in meters, and the blue line shows orientation in radians clockwise from the x-axis. Plot (b) shows the ground track produced by the same data, with the robot starting out in the lower-left.

with a two-second window. The analysis in Figure 7 did not require these small movements and was smoothed using a twenty-second window.

In Figure 5, we show 2d position and orientation data gathered during this run. Larger movements made by the balancing controller remain. Paying special attention to the blue line from plot Figure 5(a), representing the orientation of the robot, we can identify several areas of distinct holonomic motion, including in the far lower-left corner, the diagonal line in the upper-middle of the track, and the dense region at the top.

The most interesting demonstration is given in Figure 7, in which we show a direct visualization of our robot’s holonomic movement. This figure plots the robot’s orientation at a point in time against its instantaneous velocity at that time. Both orientations are measured in the world’s frame of reference. As a result, the diagonal red line drawn across

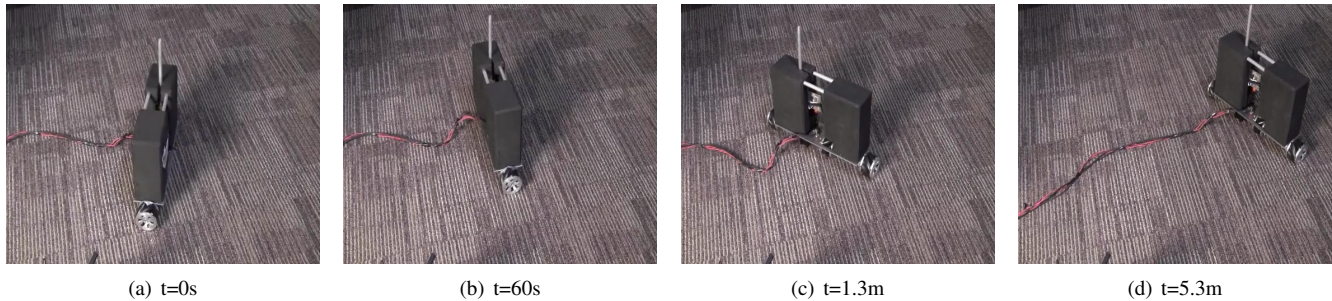


Fig. 6. Golem Wing executing holonomic motions while dynamically balancing. Starting at (a), (b) shows Wing moving laterally in the direction of its wheel axis. In (c) it rotates about a distant point and in (d) it performs forward driving.

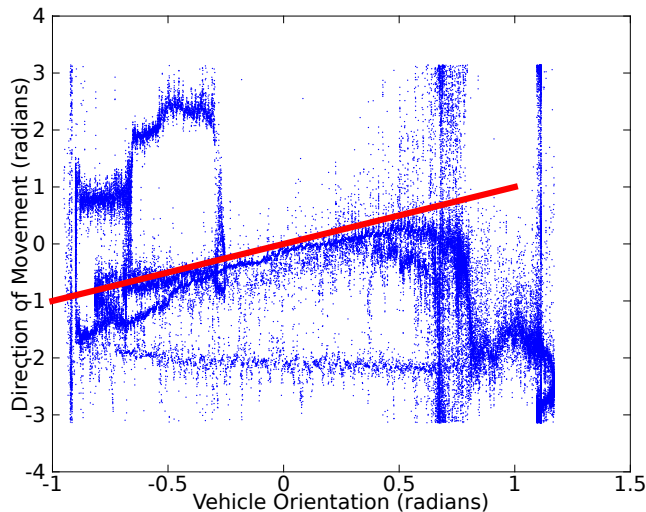


Fig. 7. A graph of the robot's orientation versus the direction it moves in. The diagonal red line represents movement directly in line with the robot's orientation.

the plot shows the possible movements for a typical vehicle that can only move in the direction that it faces. Our robot, however, is holonomic and omnidirectional, and can actuate its orientation and direction of motion independently. The dense clusters in the upper-left and lower-right are extended movements with nonequal orientation and direction, representing directionally stable holonomic movements. The line across the bottom of the plot is a movement which continues in the same direction even as the robot's orientation changes smoothly.

Our data shows that our robot is holonomic and that it remains capable of holonomic motion while balancing.

## VI. CONCLUSION AND FUTURE WORK

### A. Conclusion

This paper has presented implementation details and a controller for a holonomically-navigating and dynamically-balancing vehicle which has many of the advantages of both types of vehicles. We have also demonstrated a prototype vehicle, Golem Wing, which validates our assertions by navigating holonomically while balancing dynamically. These

abilities make it and similar vehicles compact, maneuverable, and strong platforms suitable for mobile manipulation, transportation, or movement through cramped environments optimized for human mobility.

### B. Future Work

The balancing controllers described here are intentionally rudimentary in order to simplify our demonstration. Standard improvements to mobile inverted pendulums and holonomic vehicles, such as closed-loop trajectory following, will be a subject of our future research.

## REFERENCES

- [1] Toshiyuki M. Abeygunawardhana, P. Stability Improvement of Two Wheel Mobile Manipulator by Real Time Gain Control Technique. In *Second International Conference on Industrial and Information Systems*, 2007.
- [2] M. Blackwell. The URANUS mobile robot. 1990.
- [3] N. Dantam, P. Kolhe, and M. Stilman. Equations of Motion for Dynamic Mobile Manipulators. In <http://www.golems.org/node/1050>, 2010.
- [4] Nakamura Y. Endo, T. An omnidirectional vehicle on a basketball. In *International Conference on Advanced Robotics*, July 2005.
- [5] A. Gfrerrer. Geometry and kinematics of the mecamum wheel. *Computer Aided Geometric Design*, 25:784–791, 2008.
- [6] F. Grasser, A. D'Arrigo, S. Colombi, and A. Rufer. Joe: A mobile, inverted pendulum. *IEEE Transactions on Industrial Electronics*, 49:107–114, February 2002.
- [7] Y. Ha and S. Yuta. Trajectory tracking control for navigation of the inverse pendulum type self-contained mobile robot. *Robotics and Autonomous Systems*, 17:65–80, April 1996.
- [8] K. Harada, S. Kajita, F. Kanehiro, K. Fujiwara, K. Kaneko, K. Yokoi, and H. Hirukawa. Real-time planning of humanoid robot's gait for force-controlled manipulation. In *International Conference on Robotics and Automation*, pages 616–622, 2004.
- [9] K. Harada, S. Kajita, F. Kanehiro, K. Fujiwara, K. Kaneko, K. Yokoi, and H. Hirukawa. Real-time planning of humanoid robot's gait for force controlled manipulation. In *IEEE Int. Conf. on Robotics and Automation*, pages 616–622, 2004.
- [10] K. Harada, S. Kajita, K. Kaneko, and H. Hirukawa. Pushing manipulation by humanoid considering two-kinds of zmps. In *IEEE Int. Conf. on Robotics and Automation*, pages 1627–1632, 2003.
- [11] R. Holmberg and O. Khatib. Development and control of a holonomic mobile robot for mobile manipulation tasks. *International Journal of Robotics Research*, 19:1066–1074, 2000.
- [12] K. Inoue, H. Yoshida, T. Arai, and Y. Mae. Mobile manipulation of humanoids: Real-time control based on manipulability and stability. In *IEEE Int. Conf. Robotics and Automation (ICRA)*, pages 2217–2222, 2000.
- [13] P. Kolhe, N. Dantam, and M. Stilman. Dynamic Pushing Strategies for Dynamically Stable Mobile Manipulators. In *IEEE International Conference on Robotics and Automation, 2010. Proceedings. ICRA'10, 2006*.

- [14] S. Kuindersma, E. Hannigan, D. Ruiken, and R. Grupen. Dexterous Mobility with the uBot-5 Mobile Manipulator. In *14th International Conference on Advanced Robotics (ICAR'09)*, 2009.
- [15] T. Lauwers, G. Kantor, and R. Hollis. A dynamically stable single-wheeled mobile robot with inverse mouse-ball drive. In *IEEE International Conference on Robotics and Automation (ICRA), 2006*, pages 2884–2889, May 2006.
- [16] Lauwers, T. and Kantor, G. and Hollis, R. One is enough! In *Proceedings of the 12th International Symposium on Robotics Research*, October 2005.
- [17] K. M. Lynch and M. T. Mason. Stable pushing: Mechanics, controllability, and planning. *Int. Journal of Robotics Research*, 15(6):533–556, 1996.
- [18] Franch J. Agrawal S. Pathak, K. Velocity and position control of a wheeled inverted pendulum by partial feedback linearization. *IEEE Transactions on Robotics*, 21, 2005.
- [19] A. Salerno. *Design, Dynamics, and Control of a Fast Two-Wheeled Quasiholonomic Robot*. PhD thesis, 2006.
- [20] et al. Salih, J. Designing omni-directional mobile robot with mecanum wheel. *American Journal of Applied Sciences*, pages 1831–1835, 2006.
- [21] M. Stilman, J. Wang, K. Teeyapan, and R. Marceau. Optimized Control Strategies for Wheeled Humanoids and Mobile Manipulators. In *9th IEEE-RAS International Conference on Humanoid Robots*, Paris, France, December 2009.
- [22] Mike Stilman, Jon Olson, and Will Gloss. Golem Krang: Dynamically Stable Humanoid Robot for Mobile Manipulation. In *2010 IEEE International Conference on Robotics and Automation*, Anchorage, Alaska, USA, May 2010.
- [23] T. Takubo, K. Inoue, and T. Arai. Pushing an object considering the hand reflect forces by humanoid robot in dynamic walking. In *IEEE Int. Conf. on Robotics and Automation*, pages 1718–1723, 2005.
- [24] M. Wada and S. Mori. Holonomic and omnidirectional vehicle with conventional tires. In *IEEE International Conference on Robotics and Automation*, April 1996.
- [25] R. Williams and B. Carter. Dynamic model with slip for wheeled omni-directional robots. *IEEE Transactions on Robotics and Automation*.
- [26] E. Yoshida, P. Blazevic, and V. Hugel. Pivoting manipulation of a large object. In *IEEE Int. Conf. on Robotics and Automation*, pages 1052–1057, 2005.